

Abrupt intensification of the SW Indian Ocean monsoon during the last deglaciation: constraints from Th, Pa, and He isotopes

Franco Marcantonio^{a,*}, Robert F. Anderson^b, Sean Higgins^b,
Martin Q. Fleisher^b, Martin Stute^{b,c}, Peter Schlosser^b

^a Department of Geology, Tulane University, New Orleans, LA 70118, USA

^b Lamont-Doherty Earth Observatory of Columbia University, Palisades, NY 10964, USA

^c Department of Environmental Sciences, Barnard College, New York, NY 10027, USA

Received 11 May 2000; received in revised form 2 November 2000; accepted 2 November 2000

Abstract

Sediments from western Arabian Sea core 74KL representing the last 23 ka were analyzed for helium, thorium, and protactinium isotopes. Assuming global average fluxes of extraterrestrial ³He and ²³⁰Th, the average ³He-derived sediment mass accumulation rate (MAR) is a factor of 1.8 higher than the average ²³⁰Th-derived MAR. ³He- and ²³⁰Th-derived MARs converge, however, during the Younger Dryas (YD) and during the peak of the early Holocene humid interval. These features, not seen anywhere else in the world, probably reflect a combination of climate-driven changes in the flux of ²³⁰Th and ³He. Ratios of $x_{s^{231}\text{Pa}}/x_{s^{230}\text{Th}}$, proxies of paleoproductivity, are lowest during the last glacial maximum (LGM), and increase abruptly during the Bolling–Allerod. Later, following a sudden decrease to near-LGM values during the YD, they rise abruptly to maximum values for the entire record in the early Holocene. We hypothesize that low $x_{s^{231}\text{Pa}}/x_{s^{230}\text{Th}}$ ratios reflect low productivity due to the decreased intensity of the SW monsoon, whereas the opposite is true for high ratios. The correlation between Arabian Sea productivity and monsoonal upwelling, on the one hand, and North Atlantic climate variability, on the other, suggests a linkage between high- and low-latitude climates caused by changing patterns of atmospheric circulation. © 2001 Elsevier Science B.V. All rights reserved.

Keywords: helium; thorium; protactinium; isotopes; climate change; monsoons

1. Introduction

A major component of the global climate system, the southwest Indian Ocean monsoon is the product of dynamic interactions between ocean,

atmosphere, and continent. During northern hemisphere summers, a strong pressure gradient exists between a high-pressure system over the southern Indian Ocean and a low-pressure system over the Indian–Asian continent. This gradient drives the summer monsoon circulation that, in turn, drives open ocean upwelling. The southwest Indian Ocean monsoon generates intense upwelling off the continental margins of Somalia and the Arabian Peninsula, which leads to export produc-

* Corresponding author. Fax: +1-504-865-5199;
E-mail: fmarcan@tulane.edu

tion rates among the highest in the world [1,2]. Therefore, changes in climate that alter the strength of monsoon winds can lead to direct responses in productivity. The mechanism generally called upon to explain variations in monsoon intensity over time scales of $\sim 10^4$ years, and longer, involves precessional forcing, which affects the distribution of insolation reaching the Earth [3–7]. There is a lag interval (several thousand years) for the monsoons to react to changes in insolation [7]. This lag might be caused by the long response time of the processes that are involved in translating the primary climate signal into a signal directly influencing the ocean/atmosphere forcing. Possible processes include glacial boundary conditions, e.g., changes in albedo over Asia [8] and changes in atmospheric trace gas concentrations [9].

Preserved sediments from the Arabian Sea provide an archive that can be used to reconstruct, on centennial to millennial time scales, the rela-

tionships between monsoonal variability and (1) productivity due to wind-driven upwelling and (2) eolian dust deposition onto the ocean surface. Proxy records for productivity and dust input from the Arabian Sea reveal abrupt changes on centennial to millennial time scales in the monsoon over the last two to three glacial cycles [8–13]. Several of these episodes of monsoon intensification have been correlated with climate variations in the North Atlantic [9,10].

Here we analyze sediments from Arabian Sea core 74KL [8,10]. The core was retrieved approximately 300 km from the Arabian continental margin (14°19.26' N, 57°20.82' E) at a water depth of 3212 m. Sirocko et al. [8,10] used this core to develop a high-resolution multi-proxy record for past monsoon variation over the past 24 ka. We add to this multi-proxy record by measuring the concentrations of ^{230}Th , ^{232}Th , ^{231}Pa , ^3He , and ^4He in the same sediment samples studied by Sirocko et al. [8,10]. These proxies allow us to

Table 1
He, Th, Pa data for core 74KL, Arabian Sea

| Sample | Depth (cm) | Age ^a (ka) | ^4He ($\times 10^{-7}$ cm ³ STP g ⁻¹) | $^3\text{He}/^4\text{He}$ ($\times 10^{-7}$) | $^3\text{He}_{\text{IDP}}$ ($\times 10^{-13}$ cm ³ STP g ⁻¹) | $x_s^{230}\text{Th}_o$ (dpm g ⁻¹) | ^{232}Th (dpm g ⁻¹) | Authigenic $^{238}\text{U}_b$ (dpm g ⁻¹) | $x_s^{231}\text{Pa}_o$ (dpm g ⁻¹) |
|----------|---------------|--------------------------|--|---|--|--|---|--|---|
| 74KL2 | 1.25 | 0.3 | 8.71 | 6.74 | 5.69 | 4.95 | 0.259 | 2.51 | 0.723 |
| 74KL20 | 20 | 2.3 | 1.10 | 2.51 | 2.54 | 4.47 | 0.471 | 3.94 | 0.617 |
| 74KL30 | 30 | 3.2 | 7.30 | 3.02 | 2.06 | 4.79 | 0.496 | 4.82 | 0.762 |
| 74KL67a | 67.5 | 8.3 | 5.15 | 6.96 | 3.48 | 4.51 | 0.437 | 3.38 | 0.713 |
| 74KL67b | 67.5 | 8.3 | 5.17 | 5.74 | 2.86 | | | | |
| 74KL77 | 77.5 | 9.3 | 4.68 | 1.09 | 5.02 | 4.48 | 0.407 | 3.11 | 0.668 |
| 74KL87 | 87 | 10.6 | 7.99 | 2.57 | 1.90 | 3.94 | 0.413 | 1.90 | 0.575 |
| 74KL90a | 90 | 10.9 | 6.61 | 3.02 | 1.86 | 3.73 | 0.432 | 2.44 | 0.537 |
| 74KL90b | 90 | 10.9 | 6.80 | 4.35 | 2.82 | | | | |
| 74KL92 | 92 | 11.2 | 1.07 | 2.19 | 2.13 | 3.91 | 0.427 | 2.90 | 0.707 |
| 74KL102 | 102 | 12.4 | 8.02 | 3.58 | 2.72 | 3.12 | 0.506 | 2.50 | 0.588 |
| 74KL105a | 105 | 12.7 | 1.12 | 3.52 | 3.71 | 3.26 | 0.597 | 2.89 | 0.401 |
| 74KL105b | 105 | 12.7 | 1.29 | 3.82 | 4.66 | | | | |
| 74KL107 | 107 | 13.0 | 7.97 | 3.12 | 2.33 | 3.02 | 0.488 | 2.80 | 0.394 |
| 74KL112 | 112.5 | 13.5 | 8.15 | 2.46 | 1.85 | 2.79 | 0.462 | 3.01 | 0.430 |
| 74KL117 | 117 | 14.2 | 7.72 | 2.26 | 1.59 | 2.97 | 0.504 | 2.49 | 0.484 |
| 74KL122 | 122 | 15.2 | 7.46 | 2.66 | 1.83 | 3.02 | 0.540 | 1.91 | 0.409 |
| 74KL135 | 135 | 16.9 | 1.57 | 1.43 | 1.93 | 2.79 | 0.599 | 2.24 | 0.310 |
| 74KL152 | 152 | 18.7 | 2.46 | 7.07 | 1.24 | 2.83 | 0.718 | 2.90 | 0.340 |
| 74KL177 | 177 | 20.5 | 1.42 | 1.68 | 2.10 | 2.87 | 0.730 | 3.06 | 0.339 |
| 74KL192 | 192 | 23.1 | 1.56 | 1.95 | 2.73 | 2.85 | 0.739 | 2.86 | 0.322 |

^a Age model from Sirocko et al. [8].

^b $^{238}\text{U}_{\text{authigenic}} = ^{238}\text{U}_{\text{total}} - (^{238}\text{U}/^{232}\text{Th})_{\text{detrital}} \times ^{232}\text{Th}$, where $(^{238}\text{U}/^{232}\text{Th})_{\text{detrital}}$ is assumed to be 0.7.

enhance our understanding of the variability of the western Indian Ocean monsoonal system and its effects on dust input and productivity over the last glacial cycle.

2. Methodology

Helium, thorium, and protactinium isotopes were measured in samples taken from depths of 2–192 cm in core 74KL (Table 1). This sediment interval represents approximately the last 23 ka [8]. The isotopes were analyzed for the same samples studied by Sirocko et al. [8]. A total of 18 samples were analyzed with a resolution ranging from 2 to several cm.

Helium isotopes were measured using 500-mg aliquots of sediment that were first leached with about 40 ml of 0.3 N acetic acid in order to dissolve the biogenic carbonate, which contains no helium [14]. Following this step, the residual material was washed three times with distilled water and dried to a constant weight at about 50°C. $^3\text{He}/^4\text{He}$ ratios were measured on a MAP 215-50 noble gas mass spectrometer at the Lamont-Doherty Earth Observatory (L-DEO). Details on the mass spectrometric measurement can be found in Marcantonio et al. [15,16]. Three analyses were replicated and, in general, the reproducibility of the ^4He concentrations averages 6%, while that of the ^3He concentrations averages about 24%. These reproducibilities are similar to those obtained in our previous studies [14–17].

Thorium, protactinium, and uranium (Table 1) isotopes were analyzed by isotope dilution, inductively coupled plasma mass spectrometry and α spectrometry at L-DEO. For these analyses, separate aliquots of the same samples were used as for the helium isotope measurements. The procedure for the chemical separation of Th, Pa, and U is documented in Lao et al. [18]. Initial excess ^{230}Th ($x_s^{230}\text{Th}_0$) and ^{231}Pa ($x_s^{231}\text{Pa}_0$) activities were calculated by correcting for (a) the time elapsed since sediment deposition (using ^{14}C ages [8]), (b) the presence of detrital ^{230}Th (typically 0.2 dpm g^{-1}) and ^{231}Pa (typically 0.02 dpm g^{-1}), and (c) the ingrowth by decay of authigenic uranium (typically 0.2 dpm g^{-1} for ^{230}Th and 0.02

dpm g^{-1} for ^{231}Pa). The analytical uncertainty in the thorium, protactinium, and uranium analyses is better than $\pm 5\%$.

3. Results and discussion

3.1. Constant-flux proxies and sediment mass accumulation rates (MARs)

The concentrations of $x_s^{230}\text{Th}$ and ^3He can be used as constant-flux profiling tools for determination of sediment MARs. The ^{230}Th method for estimating MARs relies on the assumption that the rain rate of particulate ^{230}Th (F_{Th}) to the ocean floor is equal to the constant rate of ^{230}Th production by ^{234}U decay in the overlying water column (see equations found in Bacon [19] and François et al. [20]). The ^3He constant-flux proxy is based on the following principles. Interplanetary dust particles (IDPs) fall onto the surface of the Earth at a rate of about 40 000 tons per year [21]. These extraterrestrial particles have $^3\text{He}/^4\text{He}$ ratios that are one to two orders of magnitude higher than material derived from the Earth's mantle or crust. Krylov et al. [22] were the first to suggest that the very high $^3\text{He}/^4\text{He}$ ratios found in deep sea sediments were due to IDP fallout onto the ocean floor. Indeed, virtually all of the ^3He found in deep sea sediments with sedimentation rates less than about 5–10 cm ka^{-1} is derived from IDPs [15,23,24]. By normalizing deep sea sediment ^3He concentrations to ^{230}Th concentrations and assuming a constant concentration of ^3He in IDPs, we have shown the global flux of extraterrestrial ^3He (and, hence, IDPs) to be relatively constant in space and time [14,15,17,25] over the last 250 ka. Within this time frame, the average ^{230}Th -normalized extraterrestrial ^3He flux over much of the globe is about $1 \times 10^{-12} \text{ cm}^3 \text{ STP cm}^{-2} \text{ ka}^{-1}$ [25], with a variation of about 50%. Farley and Patterson [26] and Patterson and Farley [27] have suggested that there is a 100-ka periodicity in the flux of ^3He to the surface of the Earth. These authors use sediment accumulation rates derived from $\delta^{18}\text{O}$ age models to calculate the fluxes of ^3He . Fluxes derived in this manner may be affected by ocean

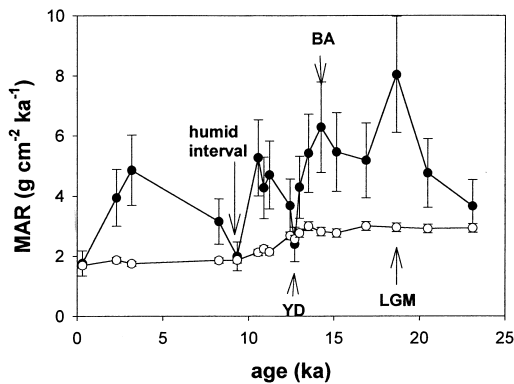


Fig. 1. ^3He -derived (solid circles) and $x_s^{230}\text{Th}$ -derived (open circles) MARs plotted versus age of Arabian Sea sediments from core 74KL. The Bolling–Allerod (BA), the Younger Dryas (YD) and the last glacial maximum (LGM) are defined by other proxies measured in this study (see Figs. 2 and 3).

dynamics (e.g., particle focusing) that tend to modulate the true IDP deposition record [17].

In regions with higher sedimentation rates and lower $^3\text{He}/^4\text{He}$ ratios, as in this study, some of the ^3He is derived from terrigenous sources ($^3\text{He}_{\text{TERR}}$). Hence, it is important to estimate the fraction of $^3\text{He}_{\text{IDP}}$ contained in the total ^3He concentration [16,26]. This value can be estimated by assuming a terrigenous $^3\text{He}/^4\text{He}$ ratio and then calculating $^3\text{He}_{\text{IDP}}$ according to equation 1 in [15]. If we assume the average crustal $^3\text{He}/^4\text{He}$ ratio of 2×10^{-8} for the terrigenous helium component in our sediment core, we obtain values for the $^3\text{He}_{\text{IDP}}$ fraction that range from 72 to 98% of the total ^3He concentration. To calculate mass accumulation rates, we use the equation $\text{MAR} = F(^3\text{He}_{\text{IDP}})/[^3\text{He}_{\text{IDP}}]$, where $F(^3\text{He}_{\text{IDP}})$ represents the global average flux of $^3\text{He}_{\text{IDP}}$ and $[^3\text{He}_{\text{IDP}}]$ the concentration of extraterrestrial ^3He derived for the sediment samples.

The average ^3He -derived MAR ($4.4 \pm 1.5 \text{ g cm}^{-2} \text{ ka}^{-1}$) is slightly lower than the average mass accumulation rate derived using the ^{14}C age data ($\sim 6.4 \text{ g cm}^{-2} \text{ ka}^{-1}$ [8]). There is a substantial (400%) short-term variability in the $^3\text{He}_{\text{IDP}}$ -derived MARs, which range from about 2 to $8 \text{ g cm}^{-2} \text{ ka}^{-1}$. The lowest $^3\text{He}_{\text{IDP}}$ -derived MARs occur at three depths, one at 2 cm, another at 77.5 cm, and another at 105 cm (Fig. 1).

Two of these depths correspond to major climate events. The 77.5-cm sample was deposited at the peak (9.3 ka [10]) of a humid interval which lasted from about 9.9 to 8.6 ka [8]. The sediment at 105 cm was deposited at approximately 12.7 ka [8], a time consistent with the Younger Dryas (YD, 11.6–12.7 ka [28]). Although Sirocko et al. [8] do not report the existence of the YD or the Bolling–Allerod (BA) in core 74KL, both events may be observed in their oxygen isotope data set, a point they acknowledge in a later publication [10].

In comparing the MARs derived by the ^3He and ^{230}Th methods, one is struck by two features (Fig. 1): (1) the ^{230}Th profiling method leads to MARs that are lower by a factor of about 1.8, on average, and which vary only by about $\pm 60\%$, from approximately 2 to $3 \text{ g cm}^{-2} \text{ ka}^{-1}$ (Table 1 and Fig. 1), and (2) there are abrupt convergences in the MARs derived from the two methods at the YD and at the peak of the early Holocene humid period. These features have not been found elsewhere [25] to date.

The lower average ^{230}Th -derived MARs could reflect: (1) lateral supply of ^{230}Th by boundary scavenging, unaccompanied by an equivalent lateral flux of IDPs, due to the fact that dissolved Th can be mixed laterally more effectively than can IDP particles, or (2) sediment focusing together with selective loss of IDPs during hydrodynamic sorting of particles carried by deep sea currents. The first possibility can be tested by measuring fluxes of ^{230}Th with sediment traps. Limited data exist in the Arabian Sea [29] that suggest that the ratio of the flux of ^{230}Th (F) to the production of ^{230}Th (P) in the water column is 1.0 ± 0.1 . This suggests boundary scavenging of ^{230}Th probably does not play a major role in the discrepancy between the MAR estimates using the two methods. However, more data are needed to determine quantitatively the magnitude of boundary scavenging of ^{230}Th in the Arabian Sea.

The ^{14}C age model allows the calculation of burial rates of both isotopes. The average burial rate of $x_s^{230}\text{Th}$ indicates an average inventory of $x_s^{230}\text{Th}$ that is 2.6 times its production rate, while the average burial rate of $^3\text{He}_{\text{IDP}}$ suggests an average accumulation rate of $^3\text{He}_{\text{IDP}}$ that is about 1.5 times its supply rate from space. These excess in-

ventories can be explained by sediment focusing. Hence, to test the second possibility, one could compare ${}^3\text{He}_{\text{IDP}}/{}^{230}\text{Th}$ ratios with Th *F/P* ratios in a suite of cores from the Arabian Sea. If IDPs are selectively lost during sediment focusing, then there should be a negative relationship between ${}^3\text{He}_{\text{IDP}}/{}^{230}\text{Th}$ ratios and Th *F/P*. Data required to test this relationship do not exist, as yet, and this will be the subject of a future study.

The abrupt convergences of the MARs derived by the two methods could reflect: (1) an increase in the supply of ${}^3\text{He}$ from another source, i.e., juvenile mantle-derived material or extraterrestrial dust originally deposited on the continents and transported to the ocean, or (2) a decrease in the selective loss of IDPs by hydrodynamic sorting due to brief declines in sediment focusing. The first possibility could be investigated by using the mineralogy and radiogenic isotope composition of the detrital phases to determine if there were changes in the source of wind-blown dust and, hence, in the direction or strength of the winds that could transport an additional source of ${}^3\text{He}$. The second possibility could be tested by analyzing grain size distributions in the sediment. While a change in this parameter across the brief intervals of convergence of MAR estimates would not prove that selective loss of IDPs had occurred, it would offer evidence for a change in currents transporting the sediments and, therefore, leave open the possibility of a change in hydrodynamic sorting.

Although the discrepancies between the helium- and thorium-derived MARs are unique, a complete explanation will require further study. If the features are attributable to sediment focusing, then they require an abrupt change in physical transport of sediment associated with the YD and with the early Holocene humid period.

3.2. Dust input

Virtually all of the ${}^4\text{He}$ and ${}^{232}\text{Th}$ in these sediments is contained within terrigenous material derived from the continents [14,16]. The relative changes in the ${}^4\text{He}$ and ${}^{232}\text{Th}$ fluxes, estimated using the ${}^{230}\text{Th}$ MARs, can, therefore, approximate the changes in the accumulation rates of

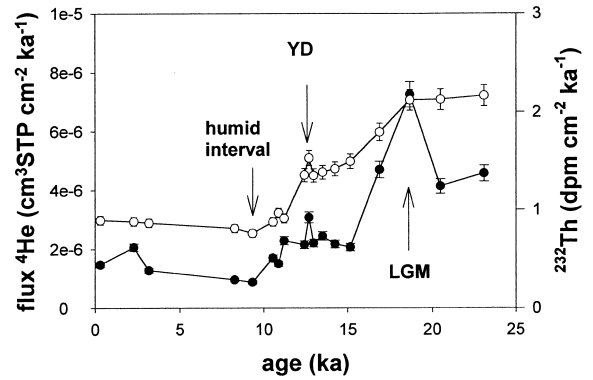


Fig. 2. Fluxes of ${}^4\text{He}$ (solid circles) and ${}^{232}\text{Th}$ (open circles) plotted versus age of Arabian Sea sediments from core 74KL. Flux of each proxy determined using the constant-flux ${}^{230}\text{Th}$ -profiling technique.

wind-blown dust from the Arabian Peninsula and Persian Gulf region. Over the last 24 ka the ${}^4\text{He}$ and ${}^{232}\text{Th}$ fluxes co-vary (Fig. 2), a relationship that is defined by a correlation coefficient (r^2) of 0.73. The higher MARs during the LGM indicate a terrigenous (${}^4\text{He}$ and ${}^{232}\text{Th}$) flux that is approximately three to five times greater than in the Holocene (Fig. 2). During the YD, there is a slight increase in the flux of terrigenous material, or at least a slowdown in the overall decay rate of this flux from the LGM to the Holocene. The YD in the Arabian Sea, therefore, marks the return of dustier LGM-like times, similar to the return to dustier conditions during the YD recorded in Greenland ice cores (e.g., [30,31]). On the other hand, during the humid interval, the terrigenous (${}^4\text{He}$ and ${}^{232}\text{Th}$) fluxes drop to the lowest values measured (Fig. 2). These low values at 9 ka are consistent with lake records from Asia and north Africa that show increased precipitation between 10 and 6 ka (e.g., [32]).

3.3. Paleoproductivity over orbital time scales

Paleoclimate proxies of productivity and dust indicate that the intensity of the SW Indian Ocean monsoon is sensitive to orbital insolation forcing at the precession period (e.g., [6,7,11,13,33–35]). Here, we also find a precessional (i.e., LGM–Holocene) signal for paleoproductivity using the $x_{\text{s}}{}^{231}\text{Pa}/x_{\text{s}}{}^{230}\text{Th}$ ratio proxy defined by Kumar et

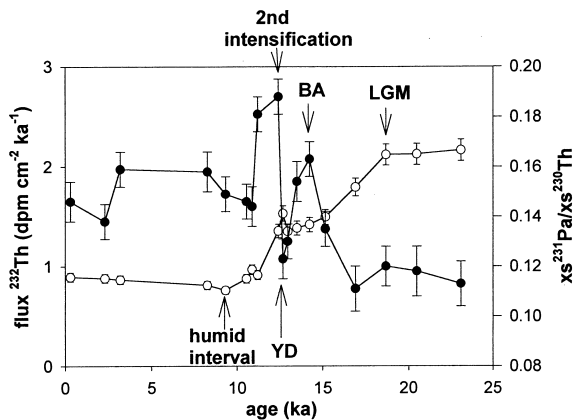


Fig. 3. $x_s^{231}\text{Pa}/x_s^{230}\text{Th}$ ratio (solid circles) and flux of ^{232}Th (open circles) plotted versus age of Arabian Sea sediments from core 74KL. Higher $x_s^{231}\text{Pa}/x_s^{230}\text{Th}$ ratios represent increased productivity, which in turn is dependent on the intensity of upwelling-favorable monsoonal winds.

al. [36,37]. In Section 3.4 we apply this proxy to suborbital millennial-scale events.

^{230}Th and ^{231}Pa are produced in the ocean from the decay of ^{234}U and ^{235}U , respectively, with an initial $^{231}\text{Pa}/^{230}\text{Th}$ activity ratio of 0.093. Whereas uranium is dissolved in seawater and, therefore, has a long oceanic residence time, both Th and Pa are particle-reactive and have relatively short oceanic residence times, much shorter than the mixing time of water in the oceans (~ 1000 years). However, Pa is not as particle-reactive as Th, so that the flux of ^{231}Pa scavenged from the water column is a function of particle flux. Indeed, analyses of Pa and Th from sediment trap studies in the modern ocean support the notion that the $^{231}\text{Pa}/^{230}\text{Th}$ ratio is mainly a linear function of biogenic particle flux [29,37,38].

The scavenging efficiency of Pa also depends on particle composition. For example, Pa is preferentially scavenged by opal [38–40], so that the $^{231}\text{Pa}/^{230}\text{Th}$ is not strictly dependent on particle flux. However, export production efficiency and, hence, particle flux are positively correlated with the abundance of diatoms in the phytoplankton assemblage [41]. This correlation between opal content of particles and particle flux provides, therefore, an important reinforcement of the general relationship between $^{231}\text{Pa}/^{230}\text{Th}$ ratios and particle flux. While $^{231}\text{Pa}/^{230}\text{Th}$ ratios are not yet cali-

brated sufficiently well to provide a quantitative measure of past changes in export production, the Pa/Th proxy should provide reliable qualitative records of past changes in productivity. In addition, this proxy has an important advantage over other paleoproductivity proxies in that it can be useful even in regions where extensive regeneration of biogenic phases and sediment focusing occur.

There is a 50% range in the Pa/Th ratios, which are all higher than the production ratio of 0.093 (Fig. 3). The higher $x_s^{231}\text{Pa}_o/x_s^{230}\text{Th}_o$ ratios may reflect a stronger monsoonal upwelling with higher productivity, whereas lower $x_s^{231}\text{Pa}_o/x_s^{230}\text{Th}_o$ ratios indicate a weaker monsoon with lower productivity. Hence, during the LGM, it appears that productivity was systematically lower than during the Holocene, consistent with previous studies [11,34,35]. Furthermore, the amplitude of the rise in Pa/Th ratios across the LGM–Holocene transition provides a scale against which rapid changes during deglacial climate events can be compared.

3.4. Paleoproductivity over suborbital time scales

In the modern Arabian Sea, respiration fueled by high surface water productivity contributes to an intense oxygen minimum zone (OMZ) 150–1200 m deep [42,43]. During the late Pleistocene, suborbital variability in sediment total organic carbon (TOC) concentrations, probably reflecting the intensity of the OMZ, correlates with $\delta^{18}\text{O}$ variations in the Greenland Ice Sheet Project 2 (GISP2) ice core, which are characteristic of the North Atlantic Dansgaard–Oeschger (D-O) cycles and Heinrich events [9].

There is disagreement over the interpretation of the northeastern Arabian Sea TOC results. This is not surprising given that factors regulating the preservation of organic matter in marine sediments have long been debated. Schulz et al. [9] argue that changes in TOC reflect changes in productivity. Because productivity in this region responds primarily to monsoonal winds, they infer that the strength of the monsoons is changing in phase with temperature changes over the North Atlantic Ocean. Strengthening of the SW Indian

Ocean monsoon increases the intensity of upwelling which, in turn, causes greater biological productivity in surface waters. Increased productivity leads to greater delivery of organic carbon to the sediments, and to a positive feedback on the TOC preserved in the sediments through increased oxygen consumption and the intensification of the OMZ. Reichart et al. [11] support the productivity interpretation of Schulz et al. [9] by showing that the TOC content of OMZ sediments is well correlated with the percent abundance of *G. bulloides*, which is an indicator of upwelling and, hence, productivity. If changes in productivity explain the changes in the TOC content, the correlation between the GISP2 and Arabian Sea records [9] points toward a linkage between low- and high-latitude climates that is governed by changing patterns of atmospheric circulation.

Schulte et al. [13] interpret the Arabian Sea TOC results differently. They infer that the TOC record is driven primarily by variable preservation of organic matter associated with variability in the intensity of the OMZ which, in turn, is caused by changes in the supply of oxygenated intermediate waters. They observe no evidence for changes in productivity in their algal biomarker data. However, %TOC is correlated with the C_{35}/C_{31} *n*-alkane ratio, a molecular biomarker correlated with organic matter preservation. Specifically, high ratios are believed to indicate better preservation under suboxic conditions in the OMZ. Hence, Schulte et al. [13] interpret the low C_{35}/C_{31} *n*-alkane ratios, together with reduced organic carbon contents, during the YD and Heinrich events to reflect the disappearance of the OMZ. High ratios during warm phases of D-O cycles are interpreted to reflect the intensification of the OMZ, and enhanced preservation of organic matter. Schulte et al. [13] believe, therefore, that the TOC record can be explained by abrupt injections of different water masses into the region of the OMZ. Specifically, during the cool YD and Heinrich events, supply of oxygen-enriched waters from the Southern Ocean into the Indian Ocean destabilizes the OMZ in the Arabian Sea. The timing of this supply of Southern Ocean waters is consistent with a weakened North Atlantic thermohaline circulation.

Distinguishing between the two hypotheses (productivity versus preservation) is crucial to making sense of how the global climate system is regulated. Further testing of the productivity hypothesis requires a proxy that is insensitive to bottom-water oxygen concentration. The $^{231}\text{Pa}/^{230}\text{Th}$ ratio is one such proxy and we use it here to help determine whether changes in productivity, which may relate to the strength of monsoon winds, have occurred over the climate reversals of the last deglaciation. Ratios of $x_s^{231}\text{Pa}_o/x_s^{230}\text{Th}_o$ are lowest during the last glacial and increase dramatically during the BA at 14.2 ka (Fig. 3). Immediately following the BA, the ratio decreases significantly during the YD (12.7 ka), and then reverts to the highest values observed at the end of YD. Values remain very high after the YD and decrease to a constant relatively high value for the rest of the Holocene. The overall increase of $x_s^{231}\text{Pa}/x_s^{230}\text{Th}$ ratios from the LGM to the Holocene occurs despite the fact that the flux of lithogenic particles (as represented by the ^{232}Th flux, Fig. 3) decreases over the same time period. This supports our contention that Pa/Th ratios respond primarily to the biogenic particle flux and, therefore, serve as a proxy for productivity and the related intensity of upwelling-favorable winds.

Our data point toward two periods of abrupt intensification of the SW Indian Ocean monsoon during the last deglaciation. These are consistent with the timing of North Atlantic climate events, one at approximately 14 ka (BA), and the other at about 12 ka, immediately following the YD. Both intensification events are more evident in our $x_s^{231}\text{Pa}/x_s^{230}\text{Th}$ ratio data than in barium concentration data [10], which suggest only a weak response to the BA–YD climate reversal. This weak response in Ba concentrations may be due to a decreased preservation of barium that is known to occur in moderately reducing sediments [44]. High authigenic U concentrations in sediments from core 74KL (Table 1) support the argument that suboxic conditions are prevalent in this region of the Arabian Sea. Whereas Ba records the longer-term rise in productivity from the LGM to the Holocene [10], it is possible that variable preservation of Ba obscured the amplitude of changes

of shorter duration, such as those that may have occurred across the BA–YD reversal.

Our interpretation of two significant episodes of monsoon intensification during the last deglaciation is in agreement with that by Overpeck et al. [45]. These authors used pollen and foraminiferal (*G. bulloides*) concentrations in cores from three Oman margin sites to show that enhanced upwelling due to monsoonal intensification took place at about 15.3–14.7 ka and then again at 11.5–10.8 ka. The timing of increased $x_{s^{231}\text{Pa}}/x_{s^{230}\text{Th}}$ ratios corresponds well with the pollen events of Overpeck et al. [45]. Furthermore, our Pa/Th record goes beyond the findings of Overpeck et al. [45] in showing that conditions during the YD returned nearly to those of the LGM. Although not seen in the pollen record [45], the amplitude of the YD reversal is evident in the TOC record [9,13]. Hence, together with the TOC data, the Pa/Th record suggests more than just an interruption of the intensification of the monsoons. Rather, one can infer that a reversal to nearly full glacial conditions occurred during the YD in the Arabian Sea.

To summarize, the $x_{s^{231}\text{Pa}}/x_{s^{230}\text{Th}}$ ratios record changes in the biogenic particle flux, which responds to increased upwelling associated with an increased intensity of the monsoon winds. These findings indicate that the rapid changes in the strength of the OMZ [9,13] are associated with changes in productivity and, hence, with changes in the intensity of upwelling-favorable monsoon winds. The BA–YD oscillation that is evident in the record of changing monsoon intensity suggests that the monsoons can be disrupted by rapid climate changes that are being forced externally (i.e., the North Atlantic).

4. Conclusions

Over the last glacial cycle, the average ^3He -derived MAR is about a factor of 1.8 higher than the average ^{230}Th -derived MAR. The reason for the discrepancy is unknown, but may be related to fractionation of the two isotopes during sediment focusing processes. If so, then the intensity of processes responsible for lateral redistribution

of sediment increased abruptly during the Younger Dryas and during the peak of the early Holocene humid interval

Ratios of $x_{s^{231}\text{Pa}}/x_{s^{230}\text{Th}}$ respond to biogenic particle flux, which, in turn, responds to intensity of upwelling-favorable monsoon winds. Abrupt changes in the intensity of the SW Indian Ocean monsoon are coincident with abrupt millennial-scale changes in the North Atlantic climate. Specifically, $x_{s^{231}\text{Pa}}/x_{s^{230}\text{Th}}$ ratios are lowest during the LGM, increase during the BA, decrease to near-glacial values during the YD, and then rise abruptly in the early Holocene to the highest values observed in the entire record. These results provide strong support for the evolving view that the precession pattern of variability of monsoon intensity is sensitive to disruption and rapid change in response to forcing by changes occurring elsewhere in the global climate system (i.e., the North Atlantic). Such a direct response on a global scale suggests that changing patterns of atmospheric circulation may be prominent forcing agents of climate.

Acknowledgements

We thank F. Sirocko for generously providing us with samples from Arabian Sea core 74KL. We are grateful to M. Frank, R. François, and F. Sirocko for constructive reviews. This work was supported by NSF Grants OCE 97-11870 and OCE 97-14898. L-DEO noble gas laboratory support was provided by the W.M. Keck Foundation and the NSF. [FA]

References

- [1] J.C. Brock, C.R. McClain, M.E. Luther, W.W. Hay, The phytoplankton bloom in the northwestern Arabian Sea during the Southwest Monsoon of 1979, *J. Geophys. Res.* 96 (1991) 20623–20642.
- [2] R.R. Nair, V. Ittekkot, S.J. Manganini, V. Ramaswamy, B. Haake, E.T. Degens, B.N. Desai, S. Honjo, Increased particle flux to the deep ocean related to monsoons, *Nature* 338 (1989) 749–752.
- [3] J.E. Kutzbach, Monsoon climate of the early Holocene, climatic experiment using the earth's orbital parameters for 9000 years ago, *Science* 214 (1981) 59–61.

- [4] W.L. Prell, Variations of monsoonal upwelling: a response to changing solar radiation, in: J.E. Hansen, T. Takahashi (Eds.), *Climate Processes and Climate Sensitivity*, Vol. 29, AGU, Washington, DC, 1984, pp. 48–57.
- [5] S.C. Clemens, W.L. Prell, Late Pleistocene variability of Arabian Sea summer monsoon winds and continental aridity: eolian records from the lithogenic component of deep-sea sediments, *Paleoceanography* 5 (1990) 109–145.
- [6] W.L. Prell, J.E. Kutzbach, Sensitivity of the Indian monsoon to forcing parameters and implications for its evolution, *Nature* 360 (1992) 647–752.
- [7] S.C. Clemens, D.W. Murray, W.L. Prell, Non-stationary phase of the Plio-Pleistocene Asian monsoon, *Science* 274 (1996) 943–948.
- [8] F. Sirocko, M. Sarnthein, H. Erlenkeuser, H. Lange, M. Arnold, J.C. Duplessy, Century-scale events in monsoonal climate over the past 24,000 years, *Nature* 364 (1993) 322–324.
- [9] H. Schulz, U. Von Rad, H. Erlenkeuser, Correlation between Arabian Sea and Greenland climate oscillations of the past 110,000 years, *Nature* 393 (1998) 54–57.
- [10] F. Sirocko, D. Garbe-Schonberg, A. McIntyre, B. Molino, Teleconnections between the subtropical monsoons and high-latitude climates during the last deglaciation, *Science* 272 (1996) 526–529.
- [11] G.J. Reichert, M. Den Dulk, H.J. Visser, C.H. Van der Weijden, W.J. Zachariasse, A 225 kyr record of dust supply, paleoproductivity and the oxygen minimum zone from the Murray Ridge (northern Arabian Sea), *Palaeogeogr. Palaeoclimatol. Palaeoecol.* 134 (1997) 149–169.
- [12] C.J. Schubert, J. Villanueva, S.E. Calvert, G.L. Cowie, U. Von Rad, H. Schulz, U. Berner, H. Erlenkeuser, Stable phytoplankton community structure in the Arabian Sea over the past 200,000 years, *Nature* 394 (1998) 563–566.
- [13] S. Schulte, F. Rostek, E. Bard, J. Rullkotter, O. Marchal, Variations of oxygen-minimum and primary productivity recorded in sediments of the Arabian Sea, *Earth Planet. Sci. Lett.* 173 (1999) 205–221.
- [14] F. Marcantonio, K.K. Turekian, S. Higgins, R.F. Anderson, M. Stute, P. Schlosser, The accretion rate of extraterrestrial ^3He based on oceanic ^{230}Th flux and the relation to Os isotope variation over the past 200,000 years in an Indian Ocean core, *Earth Planet. Sci. Lett.* 170 (1999) 157–168.
- [15] F. Marcantonio, N. Kumar, M. Stute, R.F. Anderson, M.A. Seidl, P. Schlosser, A. Mix, A comparative study of accumulation rates derived by He and Th isotope analysis of marine sediments, *Earth Planet. Sci. Lett.* 133 (1995) 549–555.
- [16] F. Marcantonio, S. Higgins, R.F. Anderson, M. Stute, P. Schlosser, E.T. Rasbury, Terrigenous helium in deep-sea sediments, *Geochim. Cosmochim. Acta* 62 (1998) 1535–1543.
- [17] F. Marcantonio, R.F. Anderson, M. Stute, N. Kumar, P. Schlosser, A. Mix, Extraterrestrial ^3He as a tracer of marine sediment transport and accumulation, *Nature* 383 (1996) 705–707.
- [18] Y. Lao, R.F. Anderson, W.S. Broecker, Boundary scavenging and deep-sea sediment dating: constraints from excess ^{230}Th and ^{231}Pa , *Paleoceanography* 7 (1992) 783–798.
- [19] M.P. Bacon, Glacial to interglacial changes in carbonate and clay sedimentation in the Atlantic ocean estimated from ^{230}Th measurements, *Isotope Geosci.* 2 (1984) 97–111.
- [20] R. François, M.P. Bacon, D.O. Suman, ^{230}Th profiling in deep-sea sediments: high-resolution records of flux and dissolution of carbonate in the equatorial Atlantic during the last 24,000 y, *Paleoceanography* 5 (1990) 761–787.
- [21] S.G. Love, D.E. Brownlee, A direct measurement of the terrestrial mass accretion rate of cosmic dust, *Science* 262 (1991) 550–553.
- [22] A.Y. Krylov, B.A. Mamyrin, Y.I. Silin, L.V. Khabarin, Helium isotopes in ocean sediments, *Geochem. Int.* 10 (1973) 202–205.
- [23] M. Takayanagi, M. Ozima, Temporal variation of $^3\text{He}/^4\text{He}$ ratio recorded in deep-sea sediment cores, *J. Geophys. Res.* 92 (1987) 12531–12538.
- [24] K.A. Farley, Cenozoic variations in the flux of interplanetary dust recorded by ^3He in a deep-sea sediment, *Nature* 376 (1995) 153–156.
- [25] S. Higgins, F. Marcantonio, R.F. Anderson, M. Stute, P. Schlosser, A global estimate of the Late Quaternary (300 kyr) IDP flux based on $^3\text{He}/\text{xs}^{230}\text{Th}$ ratios in marine sediments, *Am. Geophys. Union Trans.* 79 (1998) F50.
- [26] K.A. Farley, D.B. Patterson, A 100-kyr periodicity in the flux of extraterrestrial ^3He to the sea floor, *Nature* 378 (1995) 600–603.
- [27] D.B. Patterson, K.A. Farley, Extraterrestrial ^3He in sea-floor sediments: evidence for correlated 100 kyr periodicity in the accretion rate of interplanetary dust, orbital parameters, and Quaternary climate, *Geochim. Cosmochim. Acta* 62 (1998) 3669–3682.
- [28] P.A. Mayewski, L.D. Meeker, S. Whitlow, M.S. Twickler, M.C. Morrison, R.B. Alley, P. Bloomfield, K. Taylor, The atmosphere during the Younger Dryas, *Science* 261 (1993) 195–197.
- [29] E.-F. Yu, Variations in the Particulate Flux of ^{230}Th and ^{231}Pa and Paleoceanographic Applications of the $^{231}\text{Pa}/^{230}\text{Th}$ ratio, Ph.D. thesis, WHOI/MIT, Cambridge, MA, 1994.
- [30] K.C. Taylor, G.W. Lamorey, G.A. Doyle, R.B. Alley, P.M. Grootes, P.A. Mayewski, J.W.C. White, L.K. Barlow, Electrical conductivity measurements from the GISP2 and GRIP Greenland ice cores, *Nature* 355 (1993) 549–552.
- [31] K.C. Taylor, R.B. Alley, G.W. Lamorey, P. Mayewski, Electrical measurements on the Greenland Ice Sheet Project 2 core, *J. Geophys. Res.* 102 (1997) 26511–26517.
- [32] F. Gasse, E.V. Campo, Abrupt post-glacial climate events in West Asia and North Africa monsoon domains, *Earth Planet. Sci. Lett.* 126 (1994) 435–456.
- [33] S. Clemens, W. Prell, D. Murray, G. Shimmiel, G. Wee-

- don, Forcing mechanisms of the Indian ocean monsoon, *Nature* 353 (1991) 720–725.
- [34] G.B. Shimmield, S.R. Mowbray, G.P. Weedon, A 350 ka history of the Indian Southwest Monsoon – evidence from deep-sea cores, northwest Arabian Sea, *Trans. R. Soc. Edinburgh Earth Sci.* 81 (1990) 289–299.
- [35] M.A. Altabet, R. Francois, D.W. Murray, W.L. Prell, Climate-related variations in denitrification in the Arabian Sea from sediment $15\text{N}/14\text{N}$ ratios, *Nature* 373 (1995) 506–509.
- [36] N. Kumar, R. Gwiazda, R.F. Anderson, P.N. Froelich, $^{231}\text{Pa}/^{230}\text{Th}$ ratios in sediments as a proxy for past changes in Southern Ocean productivity, *Nature* 362 (1993) 45–48.
- [37] N. Kumar, R.F. Anderson, R.A. Mortlock, P.N. Froelich, P. Kubik, B. Dittrich-Hannen, M. Suter, Increased biological productivity and export production in the glacial Southern Ocean, *Nature* 378 (1995) 675–680.
- [38] Y. Lao, R.F. Anderson, W.S. Broecker, H.J. Hofmann, W. Wolfi, Particulate fluxes of ^{230}Th , ^{231}Pa , and ^{10}Be in the northeastern Pacific Ocean, *Geochim. Cosmochim. Acta* 57 (1993) 205–217.
- [39] H.J. Walter, M.M.R. Van der Loeff, H. Hoeltzen, Enhanced scavenging of ^{231}Pa relative to ^{230}Th in the South Atlantic south of the Polar Front: Implications for the use of the $^{231}\text{Pa}/^{230}\text{Th}$ ratio as a paleoproductivity proxy, *Earth Planet. Sci. Lett.* 149 (1997) 85–100.
- [40] M. Frank, R. Gersonde, A. Mangini, Sediment redistribution, ^{230}Th -normalization and implications for the reconstruction of particle flux and export paleoproductivity, in: G. Fischer, G. Wefer (Eds.), *Use of Proxies in Paleoceanography: Examples from the South Atlantic*, Springer-Verlag, Berlin, 1999, pp. 409–426.
- [41] K.O. Buesseler, The decoupling of production and particulate export in the surface ocean, *Global Biogeochem. Cycles* 12 (1998) 297–310.
- [42] D.B. Olson, G.L. Hitchcock, R.A. Fine, B.A. Warren, Maintenance of the low-oxygen layer in the central Arabian Sea, *Deep-Sea Res.* 40 (1993) 673–685.
- [43] U. Von Rad, H. Schulz, S.S. Party, Sampling the oxygen minimum zone off Pakistan: glacial-interglacial variations of anoxia and productivity, *Marine Geol.* 125 (1995) 7–19.
- [44] J. McManus, W.M. Berelson, G.P. Klinkhammer, K.S. Johnson, R.F. Anderson, N. Kumar, D.J. Burdige, D.E. Hammond, H.J. Brumsack, D.C. McCorckle, A. Rushdi, Geochemistry of barium in marine sediments: Implications for its use as a paleoproxy, *Geochim. Cosmochim. Acta* 62 (1998) 3453–3473.
- [45] J. Overpeck, D. Anderson, S. Trumbore, W. Prell, The southwest Indian Monsoon over the last 18000 years, *Climate Dynamics* 12 (1996) 213–225.